

## Determination of Spin-Wave Boundary Conditions by dc Effects in Spin-Wave Resonance\*

W. M. Moller and H. J. Juretschke

*Department of Physics, Polytechnic Institute of Brooklyn, Brooklyn, New York 11201*

(Received 8 May 1970)

A galvanomagnetic spin-wave experiment is described which, in conjunction with resonance absorption measurements in both uniform and nonuniform microwave fields, yields more information about the distribution of magnetization in spin-wave modes in ferromagnetic films than hitherto available, particularly for spin waves of low mode number. The method is applied to determine the spin-wave boundary conditions in 1200-Å Permalloy films, with the static field either parallel or perpendicular to the film plane. Homogeneous films show unpinned surfaces for the parallel orientation. In the perpendicular case, these films have a partly pinned film-glass interface, with anisotropies of a few tenths of 1 erg/cm<sup>2</sup>, and an unpinned film-air surface. Parallel-orientation results for a film with a thin Ni overcoat indicate the excitation of a surface mode, which is also predicted by theory.

### I. INTRODUCTION

One problem in the interpretation of standing spin-wave spectra is the nature of the boundary conditions on the transverse magnetization at the sample surfaces. Heretofore, only one type of experiment, i. e., resonance absorption in a uniform microwave field, has been commonly employed, and its interpretation can be ambiguous, particularly if the sample is inhomogeneous.<sup>1</sup> It is therefore important to augment this approach with other experiments, which give additional and more detailed information regarding the distribution of the magnetization in the excited spin-wave modes.

We have observed spin waves in Permalloy films using three experimental approaches. One is the microwave galvanomagnetic method of dc effects applied by Egan and Juretschke to the study of ferromagnetic resonance in thin Ni films.<sup>2</sup> In addition, we have measured resonance absorption in the same films in both uniform and nonuniform microwave fields. These three experiments yield three different averages of the microwave magnetization in any one spin-wave mode, since the dc effects experiment measures a time and volume average of a product of eddy current density and the magnetization, while the absorption measurements determine the oscillator strengths of the spin waves in two different field distributions.<sup>3</sup> Requiring that all three results follow from a common set of film properties establishes the boundary conditions with more certainty than would be possible on the basis of any one experiment alone.

The present work has concentrated on spin waves observed when the magnetization is parallel to the film plane, as this case presents fewer difficulties in the analysis of the dc effects experiment. The general method can also be applied when the mag-

netization lies out of plane, and some results will be presented for that case.

### II. THEORY

The full analysis of the three types of experiments rests on detailed computer calculations of both the galvanomagnetically induced dc voltages and the resonance absorption for the two field configurations. This paper can only give an outline of the exact calculations. The results so obtained, however, are similar to those following from Kittel's simple model<sup>4</sup> and we will largely employ this model to interpret the different experiments. The detailed procedures and results of the exact calculations are presented elsewhere.<sup>5</sup>

The formulation leading to the different spin-wave oscillator strengths obtained in nonuniform microwave magnetic fields and in a uniform field is well known,<sup>3</sup> but since the dc effects experiment and its possible contributions to spin-wave resonance may be unfamiliar, it will be briefly described here. In this experiment, dc electric fields and currents arise in a conducting medium undergoing magnetic resonance when eddy currents are perturbed by the precessing magnetization via galvanomagnetic effects proportional to products of these quantities. Since the eddy current and magnetization are phase related, this coupling produces dc currents and second-harmonic effects.<sup>6</sup> For example, if an 80-20 Permalloy sample carries an eddy current density  $\vec{j}$  and has static and precessing components of magnetization  $\vec{M}_0$  and  $\vec{m}$ , respectively, the coupling generates a dc electric field of the form

$$\vec{E}_0 = -(\Delta\rho/M^2)(\langle\vec{j} \times \vec{m}\rangle \times \vec{M}_0 + \langle\vec{j} \cdot \vec{m}\rangle \vec{M}_0), \quad (1)$$

where  $\Delta\rho$  is the magnetoresistance anisotropy and the inside brackets indicate an average both over time and over the sample cross section. The dc

effects, therefore, depend on a quite different average of  $\vec{m}$ , involving  $\vec{j}$  as well as  $\vec{h}$ , from that applying in absorption. It should be noted that in other materials, such as Ni, Eq. (1) also has a contribution from the extraordinary Hall effect, which introduces additional but related averages. Since this effect changes sign around the Permalloy composition,<sup>7</sup> it can be neglected here.

For a full interpretation of any spin-wave experiment it is necessary to know the fields in the sample accurately, and in the relatively thick films used for spin-wave work this must include a description of propagation effects. Four propagation modes are of importance. In a thin-film sample, for  $\vec{M}$  lying in the plane of the film, one of these modes, with  $\vec{h}$  parallel to  $\vec{M}$ , leads to the ordinary nonmagnetic skin effect. The other three modes involve solutions of an equation of motion for  $\vec{M}$ , including an exchange-anisotropy field.<sup>8</sup> We employ the Bloch equation for this description:

$$\frac{\partial \vec{m}}{\partial t} = \gamma \vec{M} \times \left( \vec{H} + \frac{2A \nabla^2 \vec{m}}{M^2} \right) - \frac{\vec{m}}{\tau}. \quad (2)$$

One of the resulting modes reduces to the electromagnetic mode of uniform precession when  $A = 0$ ; the other two represent spin waves, but only one excitation mode is resonant. For small  $A$  the propagation constants associated with the three modes can be written as power series in  $A$ . Setting  $2A/M\delta^2 = \alpha$ ,  $(\omega/\gamma + i/\gamma\tau) = \Omega$ , and  $\Omega^2 = B_{\text{res}} H_{\text{res}}$ , these series are

$$k_1^2 \delta^2 = 2i \left( \frac{B^2 - \Omega^2}{BH - \Omega^2} \right) \left[ 1 - i\alpha \frac{8\pi M(B^2 + \Omega^2)}{(BH - \Omega^2)^2} + \dots \right], \quad (3a)$$

$$k_2^2 \delta^2 = \frac{H_{\text{res}} - H}{\alpha} - i \frac{8\pi M}{BH - \Omega^2} \frac{B(H_{\text{res}} - H) + (B^2 + \Omega^2)}{B_{\text{res}} + H_{\text{res}}} + \dots, \quad (3b)$$

$$k_3^2 \delta^2 = \frac{B_{\text{res}} + H}{\alpha} - i \frac{8\pi M}{BH - \Omega^2} \frac{B(H_{\text{res}} + H) - (B^2 + \Omega^2)}{B_{\text{res}} + H_{\text{res}}} + \dots, \quad (3c)$$

where  $k_1$  refers to the quasioelectromagnetic mode and  $k_2$  defines the resonant spin wave.  $k_3$  belongs to a surface mode which in the material studied here has a skin depth of about 40 Å. The three modes make specific contributions to the fields. The electromagnetic mode gives the dominant contribution to  $\vec{e}$  and  $\vec{h}$ , and the spatial distributions of these two fields are simple since  $k_1$  is small compared to the inverse sample thickness. In Kittel's simple model the spin-wave dispersion relation is assumed to be given by the leading term of Eq. (3b), and it is the spin wave of this mode which contributes most of the transverse magnetization. Examination of detailed calculations for the fields shows that the third mode is not appreciably excited.

TABLE I. Resonant spin-wave modes in a film of thickness  $\Delta$  for five different surface pinning conditions. The modes are defined by mode number  $n (= k_2 \Delta / \pi)$  and resonance field  $H (= 4n^2)$  relative to the field at which  $k_2 = 0$ . One film surface is unpinned, the other has an anisotropy  $q$ , as defined by Eq. (4). Units of  $H$  are  $2M\Delta^2/A\pi^2$ .

Fully pinned	$n =$	0.50	1.50	2.50	3.50
$q = \infty$	$H =$	1.00	9.00	25.0	49.0
Partly pinned	$n =$	0.318	1.13	2.08	3.05
$q = \frac{\pi A}{\Delta}$	$H =$	0.404	5.12	17.2	37.2
Unpinned	$n =$	0.00	1.00	2.00	3.00
$q = 0$	$H =$	0.00	4.00	16.0	36.0
Antipinned	$n =$	0.535i	0.827	1.92	2.95
$q = \frac{-\pi A}{\Delta}$	$H =$	-1.14	2.74	14.7	34.8
Antipinned	$n =$	2.00i	0.592	1.73	2.80
$q = \frac{-4\pi A}{\Delta}$	$H =$	-16.0	1.40	11.9	31.5

To calculate all excitations we have employed the boundary conditions for  $\vec{m}$  at the film surfaces introduced by Rado and Weertman.<sup>9</sup> If  $z$  is normal to the film surfaces this requires that

$$\frac{\partial \vec{m}}{\partial z} + \frac{q}{2A} \vec{m} = 0, \quad (4)$$

where  $q$  is an anisotropy constant associated with an in-plane anisotropy. Different  $q$ 's are permitted for the two surfaces.

The above conditions together with the sample geometry determine the electromagnetic fields in the sample. In our experiments the thin-film sample is effectively a thin laterally infinite slab of material a small distance above or in contact with a shorting plane. The approximate distribution of magnetization at resonance in such a geometry has already been discussed for various partly pinned boundary conditions (finite  $q$ ) as well as for the limiting values  $q = 0$  and  $q = \infty$ .<sup>10,11</sup> In particular, it has been established that in a partly pinned film with a "hard" surface normal ( $q < 0$ ) one spin-wave excitation is a surface mode.<sup>12</sup> Table I summarizes the mode numbers and reduced resonant fields of the first four spin waves for a number of pinning conditions. As defined in the table caption, the mode numbers  $n$  can be nonintegral. The partly pinned film, of thickness  $\Delta$ , is assumed to have one surface free ( $q = 0$ ) and the other surface characterized by  $q = \pm \pi A / \Delta$  or  $-4\pi A / \Delta$ . For comparison, the modes for this surface either fully pinned or unpinned are also listed. Since there seems to be no commonly used name for the pinning associ-

ated with a hard surface normal, we will call it "antipinning." Comparison of the five cases in Table I shows that antipinning can have an appreciable effect on spreading the lowest modes apart. In fact, the surface mode can be moved arbitrarily far from the rest of the spectrum by changing  $q$ . The spectrum for the last example given is nearly linear in  $H$ , and with a proper choice of  $q$  the spacings of the first three lines can be made to be equal. Evidently a negative  $q$  can contribute to the explanation of the nonquadratic spacing of the low modes of certain films.

The  $\vec{e}$  and  $\vec{h}$  fields in the sample depend on its location relative to the shorting plane. In the "classical" resonance absorption geometry, in which the sample abuts the shorting plane, the electric field is small and the magnetic field is substantially uniform throughout the sample thickness. In the other geometry where the film is appreciably separated from the short,  $\vec{e}$ , in the lowest approximation, is uniform regardless of the properties of the film,<sup>6</sup> and  $\vec{h}$  varies linearly across the sample thickness. For the particular combination of film and geometry used in the dc effects configuration,  $\vec{h}$  has some fixed value at the front of the film, is very much smaller at the back, and is in phase with  $\vec{e}$ .

The predictions of the simple model for absorption intensities in a uniform field are well known.<sup>3</sup> Relative numerical values for the intensities of the first two partly pinned cases of Table I are presented in Table II. The case for  $q > 0$  gives intensities intermediate between those for  $q = \infty$  and  $q = 0$ . In the antipinned case the second mode is relatively strong because the main line, having an unusual distribution of  $\vec{m}$ , is only weakly excited.

Absorption intensities for nonuniform driving fields can be calculated in the same way by including in the oscillator strengths the appropriate distribution of  $\vec{h}$ . In the configuration of linearly varying  $h$  both odd and even modes of a film with two fully pinned surfaces will show absorption, and all modes will fall in intensity as  $n^{-2}$ . An unpinned film will show the  $n = 0$  mode and all odd- $n$  modes, with intensities falling as  $n^{-4}$ . If the sample's surfaces are unequally pinned, its absorption intensi-

TABLE II. Relative intensities of spin-wave resonance absorption in uniform  $h$  of two partly pinned films of Table I.

$q = \frac{\pi A}{\Delta} :$	$n$	0.318	1.13	2.08	3.05
	Intensity	1.00	0.0275	0.0029	0.00077
$q = -\frac{\pi A}{\Delta} :$	$n$	0.535 <i>i</i>	0.827	1.92	2.95
	Intensity	1.00	0.279	0.0045	0.00069

TABLE III. Relative intensities of resonance absorption of two partly pinned films described in Table I, when  $\vec{h}$  varies linearly through the film thickness. The intensities depend on whether  $h$  is largest at (a) the pinned surface, or (b) the unpinned surface.

$q = \frac{\pi A}{\Delta} :$	$n$	0.318	1.13	2.08	3.05
	Intensity (a)	1.00	0.625	0.0120	0.0144
	Intensity (b)	1.00	0.125	$5.1 \times 10^{-5}$	$2.4 \times 10^{-3}$
$q = -\frac{\pi A}{\Delta} :$	$n$	0.535 <i>i</i>	0.827	1.92	2.95
	Intensity (a)	1.00	0.121	0.014	0.018
	Intensity (b)	1.00	2.98	$1.1 \times 10^{-5}$	$6.5 \times 10^{-3}$

ties may depend strongly on which surface faces the incident microwaves. A film with one fully pinned and one unpinned surface, for example, will show an  $n^{-2}$  dependence if the pinned surface faces the microwaves, but this shifts to  $n^{-4}$  if the unpinned surface is in front. The partly pinned examples described above exhibit similar behavior, as shown in Table III. However, those modes in partly pinned films whose  $n$ 's are near even integers resemble the unexcited modes of unpinned films and fall faster with mode number than the rest.

Observation of dc effects requires a slight modification of the sample geometry. This modification is included in Fig. 1, which specifies coordinate axes and other variables of interest. The film is cut at  $x = \pm a$ , parallel to the electric field of the incident microwaves, in such a way as to block the flow of dc but not microwave currents; dc voltages can then be measured between the cuts. For computing the basic average given by the dc signal, let  $\vec{M}$  be along  $y$ , parallel to  $\vec{j}$ .

If  $\vec{m}$  has components  $m_x$  and  $m_z$ , then the electric field in the region between  $x = \pm a$  follows from Eq. (1):

$$e_{0x} = -(\Delta \rho / M) \langle j_y m_x \rangle. \quad (5)$$

Plots of  $e_{0x}$  versus  $H$ , based on exact calculations involving all modes, will be shown in Sec. IV, but the dc effects resulting from spin waves can also be predicted from the Kittel model, by using the approximate fields for a sample away from the short. The details of the line shapes depend on the relative phase of  $\vec{j}$  and  $\vec{m}$  at each  $H$ . Since at resonance  $\vec{m}$  lags behind  $\vec{h}$  and  $\vec{j}$  by roughly  $\pi/2$ ,  $\langle j_y m_x \rangle$  has the shape of a dispersion curve.

If  $j_y$  is assumed to be constant throughout the sample thickness, the absence of a signal for certain modes follows directly from the vanishing space average of  $\vec{m}$ . Thus in films with two fully pinned surfaces only odd modes produce dc effects, and calculation shows that the dc voltages developed by the odd modes vary as  $n^{-2}$ . For an unpinned film only the  $n = 0$  resonance gives rise to a dc voltage.

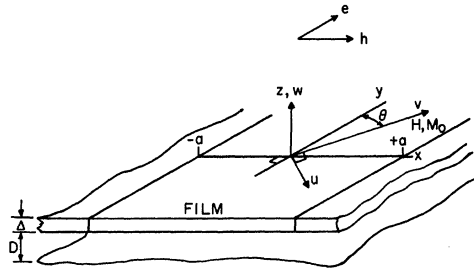


FIG. 1. Idealized experimental geometry. A film of thickness  $\Delta$  is situated a distance  $D$  above a shorting plane. Film is cut at  $x = \pm a$ .  $H$  and  $M_0$  lie in the film plane, along the  $y$  axis. The  $e$  field of the incident microwaves lies along the  $y$  axis.

A film with one fully pinned and one unpinned surface ( $n = \frac{1}{2}, \frac{3}{2}, \dots$ ) shows dc effects for all its modes; with the pinned surface facing the microwaves, the dc voltages vary as  $n^{-2} - n^{-3}/\pi$ . If the film is turned around the variation follows  $(-1)^{n+1/2} \times n^{-3}$ . Hence the interchange of the two surfaces not only affects the falloff of signal intensity but also produces an alternation in sign. Amplitudes for the partly pinned examples, given in Table IV, again show similar behavior. In the antipinned case the modes alternate in sign when the antipinned surface is in front rather than in back, because the averages of  $\vec{m}$  are opposite in sign to those of the pinned case.

If  $\vec{j}$  is significantly nonuniform, some of the signals which were excluded above will not vanish completely. As an example of practical interest, in an 80-20 Permalloy film 1200 Å thick, at the field where its  $n=1$  spin wave is resonant (200 Oe away from its main resonance), the eddy current density has a roughly parabolic variation of about 20% from front to back. This makes the  $n=1$  mode visible with an amplitude of a few percent of that of the main line. A nonuniform  $\vec{j}$  also contributes to an additional phase shift relative to  $\vec{m}$ . This phase shift determines, for instance, that  $\langle j_y m_x \rangle$  for the  $n=1$  line will have a resonance shape, in contrast to the dispersion shape of the main line.

A further test of this effect is possible because the nonuniformity of  $\vec{j}$  can be altered by rotating  $\vec{M}$  in the film plane, thus exciting the long-wavelength nonmagnetic skin effect mode. In order to analyze the result of such a rotation it is convenient to express  $\vec{j}$  and  $\vec{m}$  as components in the  $uvw$  coordinate system attached to  $\vec{M}$ , as shown in Fig. 1. Let  $m_u$ ,  $m_w$ , and  $j_v$  be quantities found in the film when the angle  $\theta$  of Fig. 1 is zero, and  $-j_u$  be found when  $\theta = \pi/2$ . Then the angular variation of the dc effects can be written

$$e_{0x} = -(\Delta\rho/M)(\langle j_v m_u \rangle \cos^3\theta - \langle j_u m_w \rangle \cos\theta \sin^2\theta). \quad (6)$$

Thus with  $j_v$  nonuniform and  $j_u$  uniform, the signals of certain spin waves will show a  $\cos^3\theta$  angular dependence and quickly vanish as  $\theta$  approaches  $\pi/2$ . Other modes will persist at large  $\theta$ , showing an angular dependence approximating  $\cos\theta \cos 2\theta$  (in the thin-film limit, where  $j_v = j_u$ ).

The analysis of this section indicates that some of the common pinning conditions can give rise to very different excitations of spin waves in the three experiments. Conversely, it should therefore be possible to identify the state of pinning on both film surfaces by an examination of the positions and intensities of the experimentally observed resonances.

### III. EXPERIMENTS

#### A. dc Effects

The experimental arrangement to detect dc effects is similar to that described by Egan and Juretschke<sup>2</sup> with some automation added. As shown in Fig. 2, microwaves from a pulsed magnetron source, with peak powers of hundreds of watts, are incident on a sample mounted in a shorted waveguide section and situated in the field of an electromagnet. dc pulses from the film are detected with a boxcar integrator, whose output is directly plotted against magnetic field. The sample geometry is that used by Egan and Juretschke.

#### B. Resonance Absorption

The resonance absorption spectrometer, designed to make measurements in the nonuniform field used in dc effects work, as well as in the usual uniform-field configuration, is shown in Fig. 3. Since in the nonuniform field the large eddy currents flowing in the film would seriously reduce the  $Q$  of a resonant

TABLE IV. Relative amplitudes of dc effects for two partly pinned films of Table I. The amplitudes depend on whether  $h$  is largest (a) at the pinned surface or (b) at the unpinned surface.

$q = \frac{\pi A}{\Delta}$		$n$	0.318	1.13	2.08	3.05
Amplitude	(a)	0.442	0.0535	0.00243	0.00125	
	(b)	0.532	-0.0305	$4.5 \times 10^{-5}$	$-7.1 \times 10^{-4}$	
$q = -\frac{\pi A}{\Delta}$		$n$	0.535i	0.827	1.92	2.95
Amplitude	(a)	0.529	-0.0968	0.00042	-0.00018	
	(b)	0.385	0.352	$8.9 \times 10^{-5}$	0.00082	

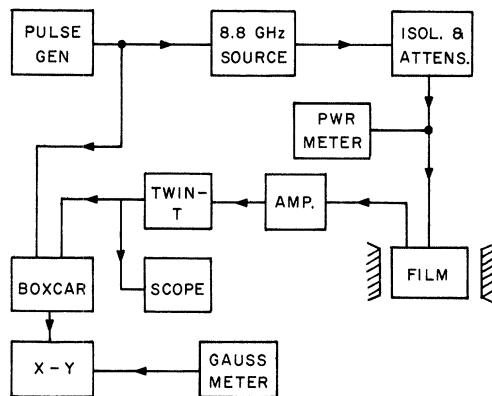


FIG. 2. Experimental arrangement of dc effects.

cavity, this spectrometer measures changes in the reflection coefficient of a shorted line containing the sample. It attains the required sensitivity through ac detection and a magic-tee bridge. Its output is the pseudoderivative of the absorption.

#### C. Auxiliary Measurements

Resistivity and low-frequency galvanomagnetic measurements on the films employ standard four-probe methods. In addition, spot checks of the films' room-temperature magnetization are made with a modification of the torque magnetometer described by Neugebauer,<sup>13</sup> by applying the balancing torque to the film with a current-carrying coil of wire surrounding the sample. The dipole moment of the coil is easy to determine absolutely and the balancing current is directly proportional to the parameter  $L/H$  used in Neugebauer's reduction of his experimental data. Film thickness is determined with a Tolansky interferometer, with an estimated error of  $\pm 20$  Å.

#### D. Film Preparation

The calculations outlined above assume that the sample is homogeneous throughout its thickness, and the preparation methods used here are designed to ensure that this is so. The source is a Permalloy charge in a BeO crucible seated in a slotted molybdenum cup and heated by rf induction. The metal charge of several grams is largely heated by radiation from the cup, whose principal purpose is to ensure that the crucible heats and cools uniformly and slowly, so as not to crack. In this way the crucible and charge can be thoroughly outgassed and reused indefinitely. The rf field leaking through the slots in the cup stirs the melt and ensures that its surface is not depleted of iron as evaporation proceeds.

The substrates are of Corning 7059 electrical glass, chosen to withstand an intense bakeout (3–4 h at 550 °C) before film growth. Films are deposited at a substrate temperature of 300 °C and ambient pressure of  $2 \times 10^{-6}$  Torr, and are annealed for 2 h at 400 °C. The electrical resistivity of the films (which is a sensitive indicator of their quality) continues to drop for at least the first hour of anneal, and reaches near-bulk values.

The vacuum system used for these depositions is a conventional glass-bell unit with a 6-in. oil-diffusion pump and unrefrigerated baffle, reaching an ultimate pressure of about  $2 \times 10^{-6}$  Torr. An indication of the degree of outgassing of the crucible is the fact that during deposition the pressure at the bell-jar base plate is only  $2\text{--}5 \times 10^{-7}$  Torr higher than ultimate.

#### IV. RESULTS FOR A UNIFORM FILM

This section presents both the experimental results and, for comparison, the corresponding exact calculations outlined in Sec. II. Those features of the calculations which can be used to determine the degree of pinning will be pointed out. In addition, the predictions of the Kittel model will be compared with both the exact calculation and experiment. Most of the experimental results refer to an 80–20 Permalloy film of 1200 Å thickness, and are typical of our findings for many films.

The appearance of a typical spin-wave spectrum, as seen by the dc effects experiment, is shown in Fig. 4. The prominent main line has a dispersion-curve shape (actually, a resonance modulated by a phase factor), as predicted by the Kittel model on the assumption that  $\hat{j}$  is nearly uniform. In addi-

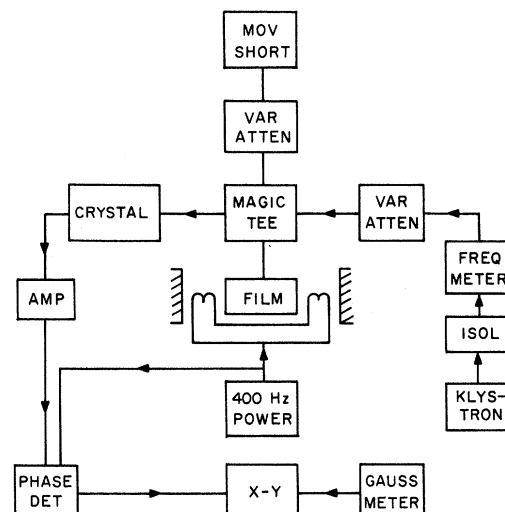


FIG. 3. Resonance absorption spectrometer.

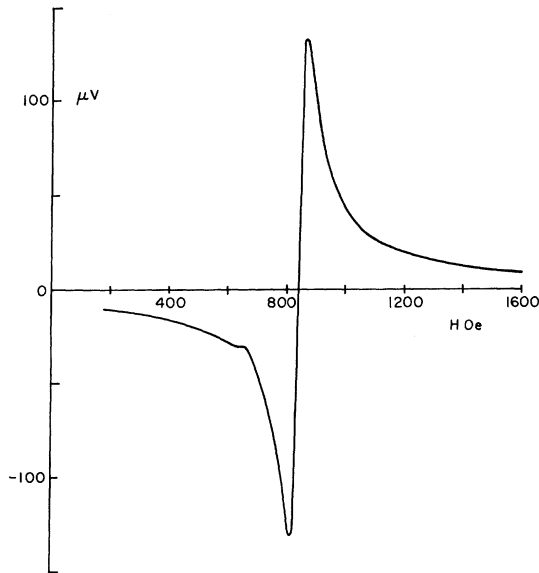


FIG. 4. Parallel orientation (dc effects) observed in 80-20 Bernalloy film 1220 Å thick. Frequency 8800 MHz,  $D=0$ , 120 cm.

tion there is a small but distinct ripple on the low-field side of the main line, which can be identified with a shorter-wavelength spin-wave mode. Figure 5 shows an exact computer calculation of  $\langle j_v m_u \rangle$  in an unpinned film having the same thickness as the experimental one and material constants listed in the caption, which are reasonable for the alloy used. The agreement as to shapes, positions, and relative amplitudes of the lines  $n=0$  and  $n=1$  is very satisfactory.

The results of Fig. 5 also can be expected on the basis of the simple model, provided one takes into account the nonuniformity in  $\vec{j}$  mentioned in Sec. II. A graph of  $\langle j_u m_u \rangle$ , in the lower part of the figure, shows no trace of the short-wavelength spin-wave peak found in  $\langle j_v m_u \rangle$ ; this reinforces the conclusion that the small observed peak is due to a nonuniform  $\vec{j}$ . The inset in the upper Fig. 5 shows the contribution of the spin-wave-mode magnetization to  $\langle j_v m_u \rangle$ ; it has roughly the size and shape predicted by the approximate model.

The experimental spectrum of the same film, as seen by resonance absorption in both uniform and nonuniform  $\vec{h}$ 's, is given in Fig. 6. The difference between the results for the two field patterns is quite striking. The uniform-field trace shows nothing but the main line, but that for the inhomogeneous field shows the higher mode quite strongly. Detailed calculations corresponding to these experiments are shown in Fig. 7; again the agreement is quite satisfactory. Furthermore, both the sim-

ple and exact calculations give the same relative intensities of the two visible lines.

The experimental data of Fig. 4 could not be explained if one were to assume that both surfaces are strongly pinned. In that case the main line would have to have the assignment  $n=1$  and the other would be labeled  $n=2$ ; another peak,  $n=3$ , would then be within the accessible field range, and would be quite conspicuous.

Regardless of the degree of pinning, the average of the transverse magnetization in the higher- $n$  spin-wave mode is always nearly zero. This may be seen easily by comparing the results of the nonuniform-field absorption experiment with either of the other two. The higher mode is negligibly excited by a uniform  $\vec{h}$  and, even when strongly excited by a nonuniform field, produces only very small dc voltages. This interpretation can be corroborated by rotating  $\vec{M}$  in the film plane towards the direction of  $\vec{h}$ . As described in Sec. II, this makes  $\vec{j}$  more uniform. The results of such a measurement are shown in Fig. 8; the high- $n$  mode dwindles rapidly in amplitude as  $\theta$  increases be-

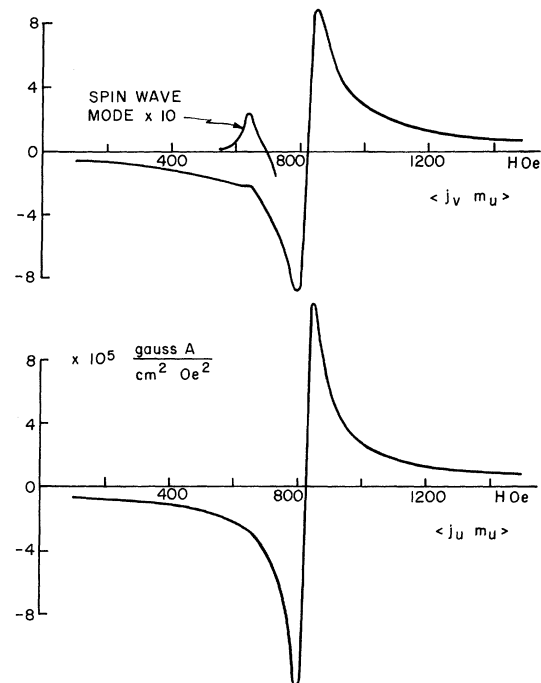


FIG. 5. Calculated dc effects in unpinned film for parallel orientation. Film parameters are thickness  $a = 1220$  Å, frequency = 8800 MHz,  $M_0 = 835$  g,  $A = 1.0 \times 10^{-6}$  erg/cm,  $\gamma = 1.81 \times 10^{-7}$  Oe $^{-1}$ sec $^{-1}$ ,  $\tau = 1.20 \times 10^{-9}$  sec,  $\delta^2 = 5.0 \times 10^{-8}$  cm $^2$ ,  $D = 0$ , 120 cm. The two curves are for  $\langle j_v m_u \rangle$  and  $\langle j_u m_u \rangle$ . The inset shows the contribution of the resonant spin-wave mode to the dc effect.

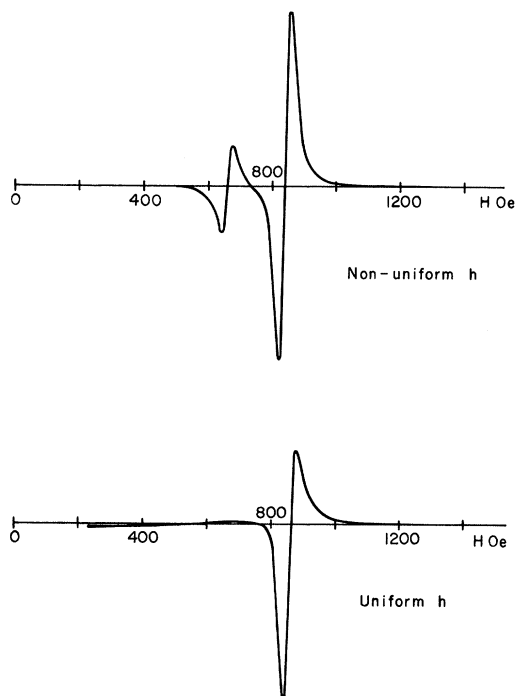


FIG. 6. Parallel resonance absorption pseudoderivatives observed in film of Fig. 4. In the nonuniform-field case  $D=0.120$  cm; the uniform-field curve has  $D \approx 0$ .

yond  $45^\circ$ . Therefore the higher modes in this film only produce dc effects when  $\vec{j}$  is nonuniform.

That the visibility of the spin-wave modes depends solely on a nonuniformity of  $\vec{j}$  (or  $\vec{h}$ ) implies that the film surfaces are equally pinned, or nearly so. One can reinforce this conclusion, also, by reversing the film in its holder and measuring the dc effects in the back-to-front position. The line shapes are found to be the same for both positions of the film, and therefore the pinning on both surfaces is the same. This point and the preceding one are covered in more detail in Ref. 5.

More precise determination of the boundary conditions, however, requires examination of less obvious features of the calculated curves. One method of analysis, which does not require that a large number of resonances be visible, is a study of the intensities of certain lines in the spectrum. For example, it was stated in Sec. II that the  $n=2$  mode of an unpinned film would not be excited in either of the two microwave fields described. If, however, the films' surfaces were partly pinned, the corresponding  $n \approx 2$  mode would be excited to some degree. That the visibility of this line is least for unpinned surfaces is confirmed by the exact calculation shown in Fig. 9. Both partly

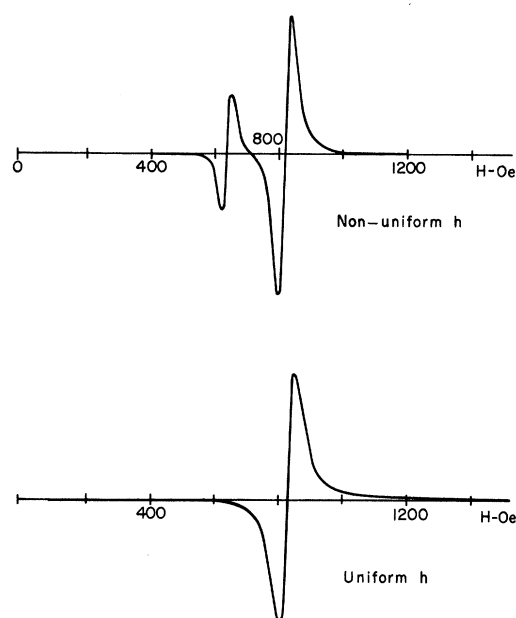


FIG. 7. Calculated parallel resonance absorption pseudoderivatives for same film parameters as in Fig. 5. For nonuniform field  $D=0.120$  cm, for uniform field  $D=0$ .

pinned curves in Fig. 9 exhibit an inflection point denoting a weak excitation of a mode near  $n=2$ , which is absent from the unpinned curve. Looking at the curves of Fig. 9 one can predict that a logarithmic derivative of  $\vec{m}$  at the surface of  $2 \times 10^4$

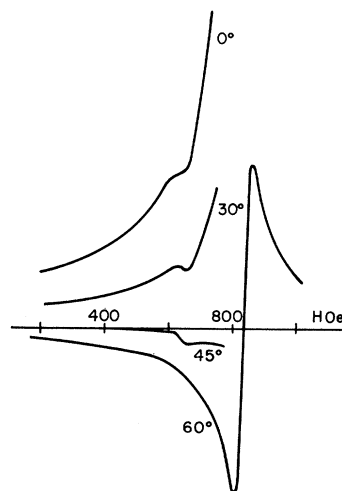


FIG. 8. Visibility of short-wavelength spin-wave dc effects in film of Fig. 4, as function of static-field angle  $\theta$ .

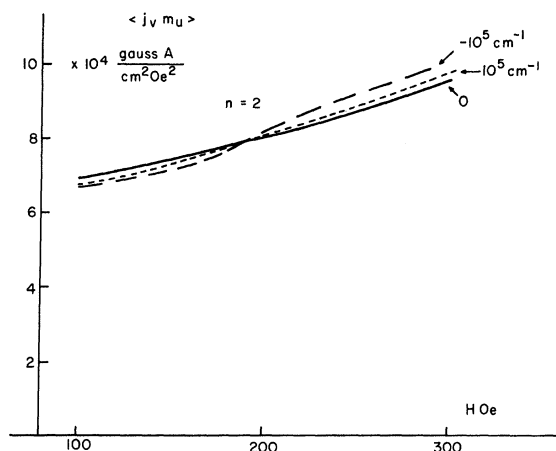


FIG. 9. Computed dc effects for  $n \approx 2$  spin wave, for various boundary conditions. Film parameters are as in Fig. 5, but with logarithmic derivatives (for both surfaces) as labeled.

$\text{cm}^{-1}$ , corresponding to a surface anisotropy of  $0.04 \text{ erg/cm}^2$ , should be detectable. Since the experimental curves show no sign of a resonance near  $n = 2$ , the anisotropy of this film must be smaller than that amount.

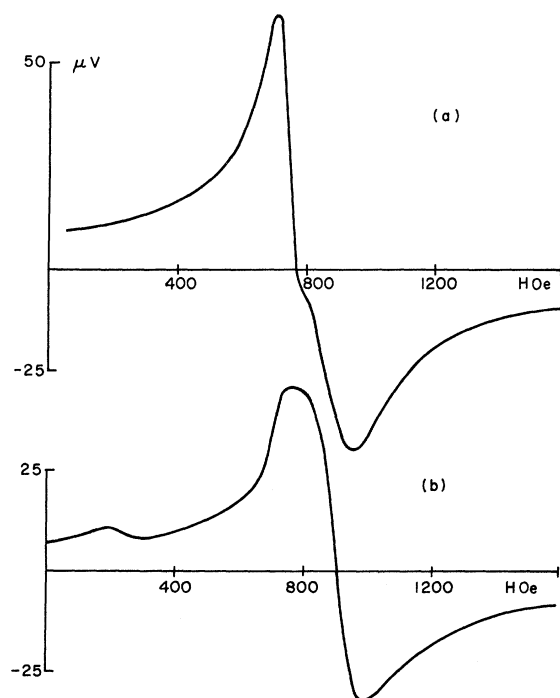


FIG. 10. dc effects observed in film similar to that of Fig. 4, but overcoated with Ni. In (a) the Ni surface is in the stronger  $h$  field; in (b) it is in the weaker  $h$  field.

## V. RESULTS FOR A COATED FILM

In an attempt to modify the boundary conditions experimentally we have deposited an overlayer of several tens of Å of Ni on a film otherwise identical to that of Fig. 4. Figure 10 shows dc effects curves for this film, for both positions of the coated surface. The results indicate that the coated surface is antipinned. Not only does the higher- $n$  spin-wave line change sign and amplitude with respect to the main line (with which it overlaps strongly) in the way predicted by the simple model, but a third line appears when the unpinned surface is nearest to the short. Furthermore, the main resonance is shifted upward in field by 60 Oe from that of Fig. 4, a quantity much greater than the normal film-to-film variation in resonant field.

Confirmation of the predictions of the simple model is contained in the detailed calculation of dc effects given in Fig. 11, based on a surface anisotropy of the coated surface chosen to match the resonant fields of the experimental film. The fit to the experiment is only qualitative, but it should be pointed out that the experimental main line is much broader than the theoretical, and that one of the approximations of the theory is the assumption of a single (Bloch-type) relaxation rate. Neverthe-

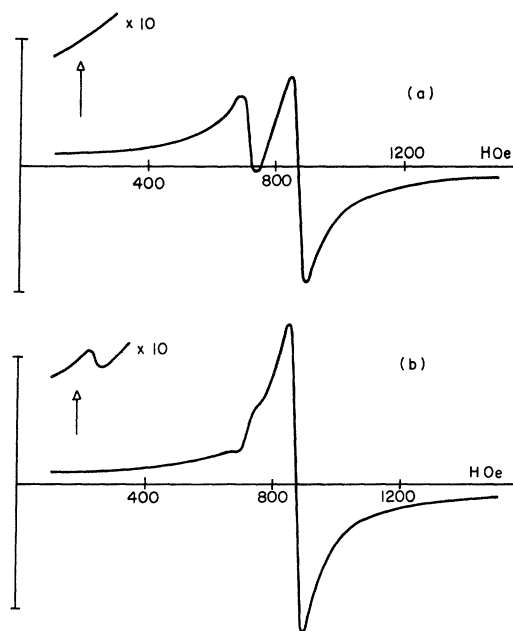


FIG. 11. Calculated dc effects for parameters of Fig. 5, but with one antipinned surface [ $(\partial m / \partial n) / m = -1.7 \times 10^5 \text{ cm}^{-1}$ ]. (a) and (b) refer to the antipinned surface oriented as in Fig. 10.



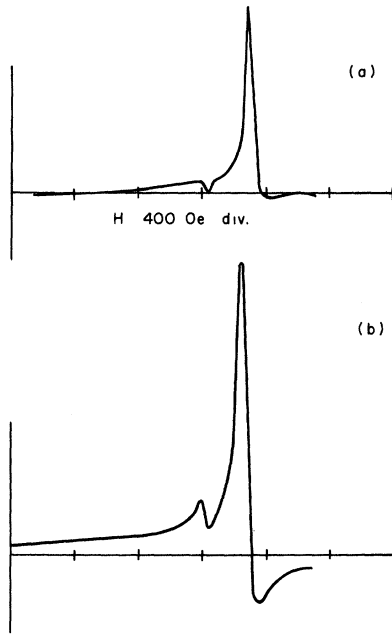


FIG. 12. dc effects observed in film of Fig. 4, with magnetization near normal to film plane.

less, theory and experiment agree on the positions of the lines and on their variations in sign and amplitude with orientation. The same agreement is found for nonuniform-field resonance absorption results.<sup>5</sup>

#### VI. OUT-OF-PLANE RESULTS

Figure 12 shows dc effects for an out-of-plane orientation of the static  $H$  a degree or two from the film normal, observed in the film of Fig. 4. The dc effects vanish when  $\vec{M}$  is strictly normal to the film plane and a detailed calculation of the spin-wave spectrum for nonnormal  $\vec{M}$  would be rather involved. Therefore these data have been analyzed only on the basis of the Kittel model.

Evidently, when the film is reversed in its holder the one visible short-wavelength mode changes sign and amplitude with respect to the main line. The surfaces are clearly differently pinned. This conclusion is confirmed by the summary of experimental and theoretical results listed in Tables V and VI. Table V lists the separations in  $H$  from the main peak of the modes visible in the experimental absorption spectrum (where more lines are visible), together with the predictions for the three cases of unpinned surfaces (for completeness only), one fully pinned surface, and the partly pinned illustrative example. No attempt at a detailed fit has been made, but the partly pinned predictions

agree well with the data and probably one could not do much better. The agreement with the partly pinned predictions is certainly better than that with either extreme case. Table VI shows the relative amplitudes, for both orientations of the film, of the observed dc effects lines, and the predictions for the same three theoretical possibilities. Once again the partly pinned values agree nicely with experiment. The sign-versus-orientation behavior of the higher- $n$  line makes the film-glass interface the pinned one, and the anisotropy associated with it is roughly  $0.3 \text{ erg/cm}^2$ . It is not clear whether the other surface is strictly unpinned or not, but the substrate interface is considerably the more strongly pinned of the two surfaces.

#### VII. CONCLUSIONS

The methods discussed here give a tool for new and detailed determination of spin-wave boundary conditions. As already mentioned, inhomogeneous-field resonance absorption has been discussed in the literature,<sup>3</sup> but it has not been fully exploited for the elucidation of boundary conditions. Clearly, the data from dc effects add an important and often decisive element to this specification. It may no longer be surprising to find that the boundary conditions on spin waves with the magnetization parallel to the film plane are appropriate to zero pinning, but the evidence presented here is more direct than that previously known and sets an upper limit to the anisotropy no larger than the Néel surface energy.

The antipinned boundary condition may occur as naturally as the pinned, depending only on the sign of the surface anisotropy. Taking this possibility into account may assist in explaining certain well-known anomalies in the spin-wave spectra of some films, since it shifts the mode spacing toward linearity and reduces the amplitude of the lowest mode in the manner of a nonuniform magnetization. In fact, antipinning could be considered the result of a localized nonuniformity in the magnetization, whose effects can be precisely calculated.

The out-of-plane results, as well, demonstrate the advantages of dc effects and nonuniform-field

TABLE V. Positions of out-of-plane spin-wave peaks, with respect to the main line, in the absorption spectrum of the film of Fig. 4, together with predictions of line positions for three possible pinning conditions ( $q_1$ ,  $q_2$ ) of the two surfaces.

	Main line	First peak	Second peak	Third peak
Observed	0	260	860	1920
(0, 0)	0	220	830	1920
(0, $\pi A/\Delta$ )	0	240	870	1920
(0, $\infty$ )	0	320	960	1920

TABLE VI. Amplitudes of out-of-plane dc effects in curves of Fig. 12, together with predictions for three possible pinning conditions ( $q_1, q_2$ ). Cases (a) and (b) refer to whether  $h$  is largest at the pinned or the unpinned surface.

(a)	Observed	1.0	$0.13 \pm 0.02$
	(0, 0)	1.0	0.0
	(0, $\pi A/\Delta$ )	1.0	0.121
	(0, $\infty$ )	1.0	0.099
(b)	Observed	1.0	$-0.06 \pm 0.01$
	(0, 0)	1.0	0.0
	(0, $\pi A/\Delta$ )	1.0	-0.057
	(0, $\infty$ )	1.0	-0.037

methods. It is difficult to decide, on the basis of conventional spin-wave resonance, whether a film's

surfaces are symmetrically pinned or, if not, which surface is pinned more strongly. With dc effects instrumentation it is a simple matter to establish the boundary conditions at both surfaces.

Finally, it is a common observation that films prepared carefully have relatively weak spin-wave spectra, with only low- $n$  modes visible.<sup>1</sup> To make full use of long-wavelength modes one must know the boundary conditions, and the techniques presented here can certainly establish them quite closely.

#### ACKNOWLEDGMENTS

H. Gärtner recommended the method of preparing the Ni overlay, and the source of proper crucibles was obtained from the Thin Films Group at CNRS-Grenoble. One of us (W. M. M.) would like to thank the NSF for Graduate Fellowship support.

\*Work supported in part by the National Aeronautics and Space Administration, Grant No. NSG-589. Based on a dissertation submitted by W. M. Moller in partial fulfillment of the requirements for the degree of Doctor of Philosophy at the Polytechnic Institute of Brooklyn.

<sup>1</sup>C. F. Kooi *et al.*, J. Appl. Phys. **35**, 791 (1964).

<sup>2</sup>W. G. Egan and H. J. Juretschke, J. Appl. Phys. **34**, 1477 (1963).

<sup>3</sup>P. Wolf, Z. Angew. Physik **14**, 212 (1962).

<sup>4</sup>C. Kittel, Phys. Rev. **110**, 1295 (1958).

<sup>5</sup>W. M. Moller, Ph. D. dissertation, Polytechnic Institute of Brooklyn, 1968 (unpublished).

<sup>6</sup>H. J. Juretschke, J. Appl. Phys. **31**, 1401 (1960).

<sup>7</sup>S. Foner, Phys. Rev. **99**, 1079 (1955).

<sup>8</sup>M. H. Seavey, Jr., Technical Report No. 239, Lincoln Laboratory, Massachusetts Institute of Technology, 1961 (unpublished), p. 2.

<sup>9</sup>G. T. Rado and J. R. Weertman, J. Phys. Chem. Solids **11**, 315 (1959).

<sup>10</sup>J. R. Hartwell, Proc. IEEE **56**, 23 (1968).

<sup>11</sup>M. Ondris and H. Gärtner, Z. Angew. Physik **24**, 200 (1968).

<sup>12</sup>V. M. Sokolov and B. A. Tavger, Fiz. Tverd. Tela **10**, 1793 (1968) [Soviet Phys. Solid State **10**, 1412 (1968)].

<sup>13</sup>C. A. Neugebauer, in *Structure and Properties of Thin Films* (Wiley, New York, 1959), p. 358.

## Two-Dimensional Ising Model in a Finite Magnetic Field\*

Michael Plischke and Daniel Mattis

*Belfer Graduate School of Science, Yeshiva University, New York, New York 10033*

(Received 26 January 1970)

We present the results of numerical calculations giving accurate estimates of the magnetization of the two-dimensional Ising model on a square lattice. Moreover, we argue that these results are strict lower bounds to the correct magnetization  $M(H, T)$ . The estimates are obtained by dividing the infinite lattice into finite strips of width between two and nine spins and infinite length. The largest eigenvalue and the corresponding eigenvector of the transfer matrix are then obtained by an iterative process. The estimates of  $M(H, T)$  converge to the correct answer for the infinite lattice everywhere except for a small region in the  $T$ - $H$  plane. We also compute isotherms and critical isobar for the corresponding lattice gas. Finally, we propose a new approximation to the transfer matrix, exactly solvable in two dimensions for  $H=0$ , which reproduces exactly the critical-point behavior of the full Ising model.

The two-dimensional Ising model has never been solved in a finite field. The critical-point exponents,<sup>1</sup> however, have all been inferred from the exact solution of Onsager<sup>2</sup> in zero field or obtained from series expansion.<sup>3</sup> It remains to determine

the magnetization  $M(H, T)$  for finite  $H$  and  $T \neq T_c$ . Recently Mattis and Plischke<sup>4</sup> derived an analytic expression for a rigorous lower bound to  $M(H, T)$  in terms of the zero-field internal energy  $u(0, T)$  and the spontaneous magnetization  $M(0, T)$ . As the